Identification of novel pathways of osimertinib disposition and potential implications for the outcome of lung cancer therapy

MacLeod, A. Kenneth; Lin, De; Huang, Jeffrey T.-J.; McLaughlin, Lesley A.; Henderson, Colin J.; Wolf, C. Roland

Published in:
Clinical Cancer Research

DOI:
10.1158/1078-0432.CCR-17-3555

Publication date:
2018

Document Version
Peer reviewed version

Title:

Identification of novel pathways of osimertinib disposition and potential implications for the outcome of lung cancer therapy

Authors

A. Kenneth MacLeod, De Lin, Jeffrey T.–J. Huang, Lesley A. McLaughlin, Colin J. Henderson* and C. Roland Wolf*.

*joint senior authors

Affiliations:

Division of Cancer Research, School of Medicine, University of Dundee, Ninewells Hospital, Dundee DD1 9SY, United Kingdom.

Running Title:

Osimertinib metabolism in humanized mice

Corresponding author:

C. Roland Wolf, Division of Cancer Research, School of Medicine, University of Dundee, Ninewells Hospital, Dundee DD1 9SY, United Kingdom. Tel +441382383134. Email: c.r.wolf@dundee.ac.uk

"The authors declare no potential conflicts of interest."

Abstract

Purpose

Osimertinib is a third-generation inhibitor of the epidermal growth factor receptor used in treatment of non-small cell lung cancer. A full understanding of its disposition and capacity for interaction with other medications will facilitate its effective use as a single agent and in combination therapy.

Experimental design

Recombinant cytochrome P450s and liver microsomal preparations were used to identify novel pathways of osimertinib metabolism *in vitro*. A panel of knockout and mouse lines humanized for pathways of drug metabolism were used to establish the relevance of these pathways *in vivo*.

Results

Although some osimertinib metabolites were similar in mouse and human liver samples there were several significant differences, in particular a marked species difference in the P450s involved. The murine Cyp2d gene cluster played a predominant role in mouse, whereas CYP3A4 was the major human enzyme responsible for osimertinib metabolism. Induction of this enzyme in CYP3A4 humanized mice substantially decreased circulating osimertinib exposure. Importantly, we discovered a further novel pathway of osimertinib disposition involving CPY1A1. Modulation of CYP1A1/CYP1A2 levels markedly reduced parent drug concentrations, significantly altering metabolite pharmacokinetics (PK) in humanized mice *in vivo*.

Conclusion

We demonstrate that a P450 enzyme expressed in smokers' lungs and lung tumors has the capacity to metabolise osimertinib. This could be a significant factor in defining the outcome of osimertinib treatment. This work also illustrates how P450-humanized mice can be used to identify and mitigate

species differences in drug metabolism and thereby model the *in vivo* effect of critical metabolic pathways on anti-tumor response.

Translational relevance

Globally, there are approximately 1.5 million new cases of non-small cell lung cancer (NSCLC) each year. Dependent on ethnicity, between 8 and 30% of these contain mutations in the epidermal growth factor receptor (EGFR) which confer sensitivity to therapy with inhibitors of this oncoprotein. Acquired resistance to first and second-generation EGFR inhibitors usually involves a further EGFR mutation, T790M. Osimertinib (AZD9291) is the most effective treatment in these latter cases and, due to its low toxicity and high level of brain penetration, is currently being explored as a first-line therapy for metastatic disease. Osimertinib is a cytochrome P450 substrate. These enzymes can define both systemic exposure and intra-tumoral drug concentrations and can therefore be major determinants in the outcome of cancer therapy. We report a novel pathway of osimertinib disposition which may be of importance in this regard.

Introduction

Lung cancer is both the most common cancer, with an estimated 1.8 million new cases in 2012, and the most common cause of mortality from cancer, responsible for 1.5 million deaths in 2012 (1). Non-small cell lung cancer (NSCLC) accounts for 80-90% of all cases. A distinct subset of NSCLC – between 8 and 30%, depending on ethnicity (2) – possess activating mutations in the kinase domain of EGFR ("EGFRm") which confer sensitivity to therapy involving "first generation" EGFR inhibitors, erlotinib and gefitinib (3,4). As with many tyrosine kinase inhibitors (TKIs), however, drug resistance emerges rapidly, with disease progression typically occurring after 9-14 months (5). The predominant mechanism of acquired resistance involves a substitution of methionine for threonine in codon 790 (T790M) in EGFR, arising through point mutation in exon 20. This mutation hinders drug binding (6) while also increasing the affinity for ATP (7), and occurs in 50-60% of patients who develop resistance to erlotinib or gefitinib (8). Several second-generation EGFR inhibitors, which target both EGFRm and T790M, have undergone clinical trial, with afatinib now approved for first-line therapy in EGFR mutation-positive NSCLC. However, the efficacy of these agents against the T790M mutant protein is disputed, as T790M emerges at a similar frequency in EGFRm+ patients treated with afatinib (9). Hence a third generation of EGFR inhibitors, designed to target both EGFRm and T790M, while sparing wild-type EGFR, is emerging.

Osimertinib is a mono-anilino-pyrimidine which covalently and irreversibly binds to cysteine 797 in the ATP binding site of EGFR, exhibiting 200 times greater potency towards $EGFRm^{/T790M}$ than $EGFR^{WT}$ (5). Compared with first and second-generation inhibitors, cell line studies demonstrated a similar activity against EGFRm, increased activity against $EGFR^{T790M}$, and an increased selectivity margin against $EGFR^{WT}$ (5). On Phase I and II clinical trial data, osimertinib was granted accelerated approval by the FDA and the EMA for treatment of metastatic $EGFR^{T790M}$-positive NSCLC which had progressed on or after TKI therapy. It was subsequently reported that the Phase III trial of osimertinib met its primary endpoint of increased progression-free survival (PFS), compared to standard platinum-

doublet chemotherapy, with evaluation of overall survival ongoing (10). Response rates to therapy are approximately 70% – of which 3% are complete and 67% partial – with a median response duration of 11.4 months as, again, resistance is acquired rapidly (11). Several mechanisms of resistance have been identified, most of which are shared with first-generation EGFR inhibitors, such as mutation of *RAS* (12), EGFR bypass through activation or amplification of *HER2/ERBB2* or *MET* (12,13) and histological transformation to small cell lung cancer (14).

Population PK analysis of clinical trial data has demonstrated the absence of an exposure/response relationship for efficacy of osimertinib across the 20-240 mg per day dose range (the prescribed dose is 80 mg per day), but a strong relationship with adverse events (15,16). In light of these data, there is significant need for studies into dose reduction and/or altered scheduling to reduce the extremely high (85% (11)) incidence of grade 1 and 2 adverse events. Moreover, further dose and schedule optimisation will facilitate the combination of osimertinib with other drugs while mitigating cumulative toxicities and forestalling resistance (17). To this end, we have investigated the *in vitro* and *in vivo* metabolism of osimertinib using recombinant cytochrome P450s, human and murine microsomal preparations, and knockout and humanized mouse lines. We identify species differences in osimertinib metabolism and demonstrate how they can be eliminated by genetic modification, and we describe novel pathways of osimertinib disposition of high relevance to the treatment of lung cancer.

Materials and Methods

Chemicals and reagents

High/low P450 activity HLM preparations from individual donors were purchased from BD Gentest (San Jose, CA, USA). Pooled human liver microsomes (150 donors) were purchased from Thermo Fisher Scientific (Waltham, MA, USA). Cloning and expression of human cytochrome P450s has been described previously (18). Osimertinib was purchased from Chemietek (Indianapolis, USA). TCDD was purchased from Toronto Research Chemicals (Canada). NADPH was purchased from Melford laboratories (Ipswich, UK). All other chemicals were purchased from Sigma-Aldrich (Poole, UK).

Animal lines and husbandry

The generation and characterisation of Cyp2cKO, Cyp2dKO, Cyp3aKO, Cyp2c/2d/3aKO, hCYP2D6*2 and hPXR/hCAR/hCYP3A4/3A7 mice has been described previously (19-22). For the humanized lines, briefly, the hCYP2D6*2 line contains a targeted insertion of an expression cassette containing 9kb of the CYP2D6 promoter, along with all exons, introns and 5' and 3' untranslated regions, into the murine *Cyp2d* locus, from which all nine functional murine *Cyp2d* genes have been deleted (20). The hPXR/hCAR/hCYP3A4/3A7 line carries a large genomic insertion of human *CYP3A4* and *CYP3A7* in place of the *Cyp3a* locus, from which seven of the eight murine *Cyp3a* genes have been deleted (21). CYP3A4 is expressed at a low basal level in this line but can be upregulated following ligand-activated nuclear translocation of the transcription factor, PXR, by RIF. In order to generate the hPXR/hCAR/3aKO line, we crossed hPXR/hCAR with Cyp3aKO animals (21). A manuscript describing the generation and characterization of the hCYP1A1/1A2 and Cyp1a1/1a2KO lines is in preparation. All animals were maintained under standard animal house conditions, with free access to food (RM1 diet, Special Diet Services, Essex, UK) and water, and a 12h light/dark cycle. All animal work was carried out in accordance with the Animal Scientific Procedures Act (1986) and after local ethical review.

***In vitro* studies**

Microsomal protein fractions were prepared as described previously (23). All incubations were performed in 100mM potassium phosphate buffer, pH 7.4, containing 3.3mM $MgCl_2$ at 37^{o}C and 300 rpm in a thermomixer. Further details are available in **Supplemental data**.

***In vivo* studies**

All animal work was carried out on 8-12 week-old male mice. Osimertinib was suspended in corn oil at 2.5 mg/mL for administration by oral gavage at 25 mg/kg (10µL per g body weight). For induction of CYP3A4 through PXR, RIF was suspended in corn oil at 1mg/mL for intra-peritoneal (*i.p.*) administration at 10 mg/kg (10µL/g body weight) once daily for three days, as described by Hasegawa *et. al.* (21), with administration of osimertinib on day four. For induction of CYP1A1 through the aryl hydrocarbon receptor (AhR), TCDD was suspended in corn oil at 1µg/mL for *i.p.* administration at 10 µg/kg (10 µL per g body weight), with administration of osimertinib 48 hours subsequently. Details of PK sample analysis are available in **Supplemental data**.

LC-MS/MS: Multiple Reaction Monitoring (MRM) analysis

Analysis of *in vitro* incubation and *in vivo* blood PK samples was carried out by UHPLC/MS-MS using a Waters Acquity UPLC (Micromass, Manchester, UK) and Micromass Quattro Premier mass spectrometer (Micromass, Manchester, UK) with Electrospray detection.

Further details are available in **Supplemental data**.

LC-MS/MS: MS^n analysis

The LC-MS/MS system consisted of a Waters Alliance 2690 HPLC system (Waters, Milford, MA, USA) and a LTQ-Orbitrap XL mass spectrometer (Thermo Fisher Scientific, Somerset, NJ, USA) with an electrospray ionization (ESI) interface. Further details are available in **Supplemental data**.

Western blotting

Microsomal fractions were adjusted to 1 mg/mL in LDS sample buffer (Life Technologies, Carlsbad, CA, USA). Primary antibodies used for immunoblotting were anti-CYP1A1 (AB1258, Merck Millipore, Billerica, MA, USA) and anti-GRP78 (ab21685; Abcam, Cambridge, UK).

Cell line studies

The A549_HO1 and H1299_HO1 cell lines will be described in detail in a future publication. Briefly, parental A549 and NCI-H1299 were obtained from the American Type Culture Collection (ATCC, Manassas, VA, USA). Genes for firefly luciferase and beta-galactosidase were introduced C-terminal to the *HO1* gene in both lines using the Transcription Activator-Like Effector Nucleases (TALEN) genome editing system. These reporter genes are separated from each other, and from *HO1*, by the 2A sequence derived from foot-and-mouth disease virus, leading to the production of a tricistronic mRNA and thereby allowing efficient production of all three proteins from the *HO1* promoter. The AREc32 cell line has been described previously (24). All cell lines were cultured in DMEM (Life Technologies) containing 10% fetal bovine serum and verified as mycoplasma-free (MycoAlert, Lonza, Basel). For induction studies, cells were exposed to osimertinib in complete medium for 24h and luciferase activity measured using a commercially available kit (Promega, Madison, WI, USA).

Data analysis

Spearman's rank correlation coefficients were calculated in Microsoft Excel (Microsoft, Redmond, WA, USA). PK parameters of *in vivo* data were calculated with a simple non-compartmental model using the PK Functions package in Microsoft Excel and *p* values were calculated using an unpaired, two-tailed *t*-test. *: $p = <0.05$, **: $p = <0.01$, ***: $p = <0.001$.

Results

In vitro *metabolism of osimertinib: similarities and differences between human and mouse*

In order to determine the suitability of the mouse as a model system to investigate pathways of osimertinib disposition *in vivo*, we first compared the metabolism of this drug in mouse and human liver microsomal fractions *in vitro*. Analysis of samples from incubations with HLM and wild-type MLM identified two demethylated (designated DM-1 and -2) and five hydroxylated (designated OH-1 to -5) metabolites in each species (**Figure 1A and B**). The demethyl-osimertinib profile was closely-matched between species (**Figure 1C**). However, the hydroxylated forms were produced at very different ratios, and two were produced in much greater quantities by MLM (**Figure 1D-E**). Manual fragmentography confirmed that the seven metabolites produced by MLM were the same as those produced by HLM, and that DM-1 and DM-2 are the previously reported clinically-important AZ5104 (M6) and AZ7550 (M3) metabolites, respectively (**Supplementary Figure 1**) (25,26). The structure of osimertinib and sites of modification are shown in **Figure 1F**. In previous reports, only three mono-hydroxylated metabolites have been identified (25,26). OH-4 corresponds to M1, but structural detail for the other two previously identified metabolites – designated M4 and M7 – are unavailable for comparison with our data (25,26).

To further clarify the human cytochrome P450s involved in osimertinib metabolism we carried out incubations with a panel of recombinant P450 enzymes. CYP3A4 and CYP1A1 were the most active in generating DM-1, exhibiting approximately equivalent activity (**Figure 2A**). CYP3A4 played a major role in generating DM-2, with minor roles for CYP1A1 and CYP2C8 (**Figure 2B**). Interestingly, CYP1A1 had by far the highest activity in forming the OH-1,OH-3 and OH-5 metabolites (**Figures 2C, 2E and 2G**), while CYP1A2 and, to a lesser extent, CYP3A4, CYP1A1 and CYP2C8 produced OH-2 (**Figure 2D**). CYP3A4 was most active in the generation of the 4-OH metabolite (**Figure F**).

In order to establish which cytochrome P450s play a predominant role in the production of these metabolites in human liver we used a panel of HLM from 15 donors, characterised in their activity towards probe substrates for individual P450 isoforms. The formation of DM-1 correlated strongly with that of 6β-hydroxy-testosterone, the marker for CYP3A4, agreeing with the recombinant protein data (**Supplementary Table 2**). There was also a strong correlation with CYP2A6 activity but we deemed this potentially artefactual as CYP3A4 and CYP2A6 probe activities within the HLM panel correlate (not shown). This relationship has previously been observed in a separate panel of HLM samples (27). Indeed, recombinant CYP2A6 did not produce this metabolite (**Figure 2A**). It should be noted however that Dickinson *et al* observed some activity of recombinant CYP2A6 with osimertinib (26). Formation of DM-2 in the HLM panel agreed less well with the recombinant protein data, as correlation with CYP3A4 activity was considerably weaker than with CYP2A6, CYP2B6 and CYP2C8. OH-1 data were consistent as, in the absence of a reference CYP1A1 activity in the HLM panel, CYP3A4 was the next strongest correlation (disregarding CYP2A6). Generation of OH-2 correlated well with CYP3A4 and CYP2C8 activities, consistent with the recombinant data but, in stark contrast, the predicted CYP1A2 correlation was not observed. The reason for this is unclear. Consistent with the recombinant P450 data, the correlation of OH-4 formation with CYP3A4 activity was highest. This analysis did not clearly identify the enzymes involved in the formation of the OH-3 and OH-5 metabolites (**Supplementary Table 2**).

In addition to the recombinant protein and probe substrate correlation analyses, we further characterised the P450s involved in osimertinib disposition using isoform-specific inhibitors in pooled HLM. In broad agreement with the above work, the generation of DM-1, DM-2, OH-1 and OH-2 were strongly inhibited by the CYP3A4 inhibitor ketoconazole (**Supplementary Table 3**). Further, in agreement with the correlation analysis, inhibition of CYP1A2 did not alter production of OH-2. Due to the reported low basal level of expression of CYP1A1 in human liver (28), we did not attempt to inhibit this enzyme in HLM.

To further characterise the involvement of CYP3A4 and CYP1A1 in osimertinib metabolism, we determined the apparent kinetic parameters for conversion to DM-1, DM-2 and OH-1 by recombinant forms of these enzymes *in vitro*. All data were in agreement with the above: (i) both CYP1A1 and CYP3A4 generated DM-1, with the former demonstrating a far lower K_M and the latter demonstrating a higher V_{max}, (ii) CYP1A1 was essentially inactive in the formation of DM-2 with CYP3A4 exhibiting significant activity (iii) both enzymes generated OH-1, but CYP1A1 had both a lower K_M and higher V_{max} (**Supplementary Table 4**).

Osimertinib is an irreversible inhibitor of EGFR containing an acrylamide reactive centre which binds covalently to cysteine 797 in the kinase active site (5). Specificity for this target is enhanced through the formation of two hydrogen bonds between the pyrimidine core of osimertinib and methionine 793 of EGFR. This alpha/beta unsaturated ketone moiety is thiol-reactive (29), a common feature of many activators of the transcription factor nuclear erythroid 2 related factor 2 (NRF2). NRF2 provides a primary defence against reactive electrophiles and has been associated with drug resistance in cancer (30). We therefore tested the ability of osimertinib to activate NRF2-driven luciferase reporters in three stable cell lines; two driven off the endogenous heme oxygenase 1 (HO1) promoter, A549_HO1 and H1299_HO1, for which NRF2 is one of a number of regulators, and one driven off a synthetic promoter containing eight copies of the antioxidant response element (ARE), which is specific for NRF2, AREc32 (24). In each cell line, treatment with 3 μM osimertinib for 24 hours (a non-toxic dose, as determined by ATP cytotoxicity assay over 72 hours, data not shown) activated the reporter 2- to 3-fold (**Supplementary Figure 2**).

Murine Cyp2d are responsible for the species difference in osimertinib metabolism

As described by Cross *et al*, the half-life of oral clearance of osimertinib is approximately three hours in the mouse (5). However, in early clinical studies, the human value was found to be approximately

50 hours, "longer than would be predicted from the preclinical data". The *in vitro* metabolic stability of osimertinib in HLM was much greater than in MLM (**Figure 3A**). To determine the reason for this species difference in metabolism, we analysed osimertinib stability in liver microsomes from *Cyp2c*, *Cyp2d* and *Cyp3a* gene cluster knockout mice, and from a combined *Cyp2c/2d/3a* triple-cluster knockout line (19-22). Osimertinib stability was greatly increased in *Cyp2d* KO (**Figure 3A**) and *Cyp2c/2d/3a* KO (not shown) microsomes but not in any of the other KO microsomes. The production of the major OH-2 metabolite was also concomitantly decreased (**Figure 3B**). These data demonstrated that unlike in human samples, murine hepatic Cyp2d enzymes were responsible for osimertinib metabolism and that this defines a major species difference in the pathway of disposition. To establish whether this was also the case *in vivo*, and responsible for the short half-life of osimertinib in mice *in vivo*, we compared the PK profile of wild-type animals to those humanized for CYP2D6, which carry the human enzyme in place of the murine Cyp2d cluster. Consistent with the *in vitro* data, in the humanized mouse model a profound change in osimertinib disposition was observed. The drug was cleared within 32 hours of administration to wild-type mice, yet remained detectable in serum from h2D6 animals 80 hours after administration (**Figure 3C**). Exposure ($AUC_{0\text{-}t}$) and $t_{1/2}$ were 5.3-fold and 2.80-fold higher, respectively, in the humanized animals, while Cl decreased 6.1-fold (**Supplementary Table 5**). Consistent with this, and with the *in vitro* data, the circulating OH-2 metabolite was also greatly decreased in the humanized line (**Figure 3D**).

Osimertinib disposition following the induction of CYP3A4 in humanized mice in vivo

In humans, osimertinib is predominantly metabolized by CYP3A4 in the liver (25,26,31). We therefore investigated the role of this enzyme to osimertinib disposition in the humanized hPXR/hCAR/h3A4 mouse line *in vivo*. In order to induce hepatic CYP3A4 expression in this line, animals were pre-treated with the PXR activator, RIF. To definitively attribute any effects observed to CYP3A4 – i.e. to rule out any effects of this inducing agent on, for example, drug transporters (23), we also carried out the analysis on a novel mouse line humanized for PXR and CAR, on a Cyp3a-

knockout background. In the hPXR/hCAR/h3A4 line, pre-treatment with RIF significantly decreased exposure to osimertinib, with a 2.4-fold decrease in AUC_{0_t} and a 2.1-fold decrease in C_{max} (**Figure 4A and Supplementary Table 6**). This decrease was due to the activity of CYP3A4, as no change was observed in the hPXR/hCAR/3aKO line with RIF pre-treatment **(Figure 4B).** Notably, both of the mouse models utilized here retain the *Cyp2d* gene cluster, hence the PK profile is more similar to wild-type mice than to h2D6.

In humans, CYP3A enzymes have been reported to be primarily responsible for both the generation and the further metabolism of the key active metabolites, DM-1 (AZ5104) and DM-2 (AZ7550) (25,26,31). In the humanized model exposure to DM-1 decreased to a similar extent in both mouse lines after RIF pre-treatment (**Figure 4C,D**). This pattern was also apparent for DM-2, although was less well-defined due to the low signal intensity (**Figure 4E,F**) suggesting that Rif induces a non-CYP3A4 route of disposition of these metabolites, possibly through the induction of drug transporters.

Osimertinib is a substrate and inducer of CYP1A1 in vivo

Pre-clinical data on the metabolism of osimertinib did not identify CYP1A1 as a catalyst of osimertinib metabolism (25,26,31,32). As described above, recombinant CYP1A1 protein was highly active in generating DM-1, OH-1 and OH-5, and moderately active in generating DM-2, OH-2 and OH-3 (**Figure 2, Supplementary Table 4**). These data are potentially important in relation to the outcome of osimertinib therapy as CYP1A1 is highly expressed in the lungs of smokers, and also in lung tumors (33). To explore the influence of CYP1A enzymes on osimertinib disposition *in vivo* we carried out pharmacokinetic analysis in novel Cyp1a1/1a2 knockout and CYP1A1/1A2 humanized mouse lines. The basal expression of CYP1A1 in the h1A1/1A2 line is low (Kapelyukh *et*. *al*., manuscript in preparation), however it can be induced in a number of tissues including liver, lung and small

intestine by exposure of the mice to TCDD, an activator of the Ah receptor (Ahr). In h1A1/1A2 mice pre-treated with TCDD, there was a 3.4-fold decrease in $AUC_{0\text{-}t}$ and a 3.3-fold decrease in C_{max} of osimertinib (**Figure 5A and Supplementary Table 7**). There was no change in exposure in the 1a1/1a2KO line. Correspondingly, TCDD-pre-treatment greatly increased circulating levels of the OH-1 metabolite in humanized mice, but had no effect in knockouts (**Figure 5B**). In this experiment, TCDD-mediated activation of Ahr occurred in several tissues – liver, small intestine and lung (Kapelyukh *et. al.*, manuscript in preparation) – hence the effects on osimertinib and metabolite disposition were likely to be driven by a combination of hepatic, intestinal and pulmonary CYP1A1/1A2. In order to test whether induction of these enzymes in lung could alter osimertinib metabolism specifically in this tissue, we carried out *in vitro* studies using lung microsomes from h1A1/1A2, 1a1/1a2KO and wild-type animals, both with and without TCDD-pre-treatment (two days prior to harvest). Induction of CYP1A1/1A2 in pulmonary microsomes from humanized animals increased OH-1 generation (**Figure 5C**). Interestingly, there was no increase in OH-1 generation in samples for pretreated wild-type animals (**Figure 5C**). There were, however, far greater increases in OH-3 (**Figure 5D**) and OH-5 (**Figure 5E**) production in lung samples from wild-type relative to h1A1/1A2 mice. As substrates of CYP1A1 are typically found also to be inducers of this enzyme, we administered osimertinib once daily for four days to h1A1/1A2 mice. Livers were harvested on day five and CYP1A1 protein levels assessed by Western blot **(Figure 5F)** and EROD activity **(Figure 5G)**. Increases in both indicated that this drug is indeed an inducer of CYP1A1 *in vivo*.

Discussion

Lung cancer is a global problem with high incidence and mortality. It is largely refractive to conventional chemotherapy and, despite large numbers of clinical trials and advances in stratification facilitated by increasing histopathological subdivision, outcomes are poor. Recently, patients with activating mutations in EGFR have benefited from therapy with the first generation EGFR inhibitors erlotinib and gefitinib (3,4). However, resistance to these therapies rapidly emerges, with the T790M mutation in EGFR representing the predominant mechanism of innate/acquired resistance (8). Second generation EGFR inhibitors designed to target this mutant protein exhibit significant side effects indicative of widespread inhibition of wild-type EGFR. As a consequence, the third generation of EGFR inhibitors has been designed with a higher level of specificity against the mutant forms of EGFR (5,34). However, resistance to these drugs still emerges rapidly, the tumoral mechanism of which appears similar to those identified for the first-generation inhibitors (12-14). In this work we have identified and modeled, in humanized mice *in vivo*, the key metabolic factors which determine osimertinib disposition.

The half-life of oral clearance of osimertinib in wild-type mice is approximately three hours, yet, in the first human patients with confirmed radiographic response, half-life was observed to be approximately 50 hours, "longer than would be predicted from the preclinical data" (5). We have shown this species difference is due to the extremely high activity of enzymes in the murine *Cyp2d* gene family. Conversely, the human CYP2D6 homolog has minimal activity towards osimertinib. Knockout of the murine *Cyp2d* gene cluster (and humanization for *CYP2D6*) therefore renders both the *in vitro* metabolic stability and the *in vivo* PK profile of this drug much more representative of that observed in humans.

Unlike in mice, the primary pathway of osimertinib metabolism in patients is mediated by CYP3A enzymes (25,26,31). Indeed, prescribing guide lines advocate the avoidance of co-administration of

strong CYP3A4 inducers. In clinical trials, the AUC_{ss} of osimertinib was reduced by 78% when combined with the CYP3A4 inducer rifampicin (35). We found that, in humanized PXR/CAR/CYP3A4 mice, rifampicin pre-treatment also decreased osimertinib $AUC_{0\text{-}t}$ by 58% and through the use of Cyp3a-knockout animals we confirmed that this was due to CYP3A4 induction. The osimertinib dose in our experiments gave a C_{max} of 123.6 ng/mL and an AUC_{0_t} of 1144 hr*ng/mL. In humans, at the prescribed dose of 80 mg once daily, $C_{max,ss}$ was 311.7 ng/mL (623.8 nmol/L, range: 167-2100, CV: 53.84%)) and AUC_{ss} was 5960 hr*ng/mL (11930 nmol*hr/L (range: 3650-38900, CV: 51.77%)) (15). Hence, although our studies gave levels of exposure in the lower range of clinically-observed values, the quantitative similarity with the human data demonstrate that CYP3A4-humanized animals provide a powerful model for the prediction of CYP3A4-mediated effects on human PK and drug efficacy.

Metabolism by CYP3A4 generates two pharmacologically active metabolites, AZ5104 and AZ7550 (here referred to as DM-1 and DM-2, respectively), which have selectivity profiles similar to parent compound, although the former is less specific for T790M (25,26,31). These metabolites are, themselves, further metabolized by CYP3A4/5. In our study, pre-treatment with rifampicin decreased exposure to AZ5104 and AZ7550 in both mouse lines. These data suggest that RIF is acting through PXR, to induce a novel CYP3A4–independent pathway involved in disposition of these pharmacologically active metabolites, possibly through the induction of the drug transporters.

Although CYP3A4 is reported to be the major enzyme responsible for osimertinib metabolism, it is important to note that intra- and inter-individual variability in the hepatic levels of this enzyme can be as high as 60-fold (27). In this paper, we report the identification of a further novel pathway of osimertinib metabolism involving CYP1A1 and that suggest that this enzyme may also play an important role in both osimertinib disposition and in its efficacy. CYP1A1 generated both the demethylated and hydroxylated metabolites of osimertinib and, indeed, had the highest activity in the generation of OH-1, OH-3 and OH-5 metabolites. CYP1A1 is a highly inducible enzyme in almost

all tissues as a consequence of activation of the AhR, most notably by the polycyclic aromatic hydrocarbons (PAH) found in cigarette smoke (28,33). Further, it is often expressed at significant levels in tumors (36). CYP1A2 is considered more liver-specific, but its promoter contains an element responsive to PAHs (37) and phenotypic assays are indicative of its induction with smoking (37,38). Induction of CYP1A1 and CYP1A2 as a consequence of smoking alters the disposition of a wide variety of drugs and, in some cases, this interaction requires dose adjustment or a change in the drug prescribed (39).

CYP1A1-mediated metabolism is of particular relevance to the treatment of lung cancer, as this enzyme may metabolize drugs within lung tumors or may alter drug exposure due to metabolism in the adjacent lung tissue. This possibility is exemplified by our finding that *in vitro* incubation of osimertinib with lung microsomes following the activation of AhR and the induction of CYP1A1, led to greatly increased production of the OH-1 metabolite, with some increase in the OH-3 or OH-5 osimertinib metabolites. Intra-tumoral osimertinib metabolism could affect both drug and metabolite levels and therefore contribute to individual patient responses or indeed drug resistance.

The induction of CYP1A1 in the lung has also been shown to alter drug exposure (40). In the case of the CYP1A substrate, erlotinib, a dose adjustment is recommended in smokers to counteract the increased clearance mediated by CYP1A1/1A2 (41). Recently, Phase I clinical trial of a combination of erlotinib with dovitinib had to be halted due to a high incidence of grade 3 toxicity and a profound drug-drug interaction (DDI), stemming from dovitinib acting as a CYP1A1/1A2 inducer (42). Using a novel CYP1A1/1A2 humanized mouse line, we found that induction of these enzymes following systemic activation of AhR greatly decreased exposure to osimertinib. Brown *et al*, in a population PK analysis of 778 patients, found that smoking status (current smokers=3%, former smokers=30%, never smokers=67%) did not have a significant effect on osimertinib PK (dose-normalized AUC_{ss}) concluding that CYP1A1 induction does not have a major effect on metabolism (16). However, the very small number of current smokers in this study, and the fact that these data were not analysed in relation to when smoking cessation occurred, makes interpretation of the potential effects on

osimertinib pharmacokinetics unclear. This is an important issue in relation to our work, since when patients stop smoking is a key factor in determining CYP1A1 levels. In normal lung tissue of patients who stop smoking, CYP1A1 levels begin to decrease after two weeks, becoming undetectable after six weeks (33). Initially, the labelling of osimertinib recommended the avoidance of co-administration of substrates of CYP1A due to potential induction of CYP1A2 (25,32). This recommendation was removed from the label in August 2016, without explanation (35). Our data suggest that the interaction of osimertinib with CYP1A1/1A2 could have significant effects on its therapeutic efficacy. We have examined the AURA clinical trial data, including the recently published FLAURA study, to evaluate evidence that smoking is a factor in the outcome of therapy. This has not been possible because detailed information on smoking history - in particular, time from cessation in relation to the initiation of treatment - was not reported. This information should now be gathered as part of the approved clinical use of osimertinib.

During clinical trial of osimertinib, the 80mg per day dose level was selected for evaluation in Phase 2 as, above this level, incidence and severity of adverse events increased (15). There is no evidence of an exposure/response relationship for efficacy across the 20-240 mg dose range. There is however a strong relationship between dose and toxicity, with higher exposure resulting in increased likelihood of rash, diarrhea – adverse events indicative of the inhibition of wild-type EGFR – or elongation of the QTc interval (15,16). Therefore, it would appear that a dose reduction is feasible, and might reduce the high incidence of grade 1 and 2 adverse events (85% (11)) without loss of efficacy. At steady-state, inter-individual variability in osimertinib PK is high: the coefficient of variation for C_{max} is 54%, while for $AUC_{0\text{-}t}$ is 52% (43). Individuals at either end of the spectrum may be greatly under- or over-exposed to drug. Much of this variability in exposure may be driven by variability in CYP3A4 and CYP1A1 expression levels. Notably, Brown *et al* identified ethnicity as a covariate for AUC of the CYP3A-generated metabolite, AZ5104 (DM-1), with lower levels observed in non-Caucasian patients, including Japanese (16). One possible explanation for this may be the lower

level of CYP3A activity in Japanese men than in European American men (44), should this be found also to be the case in the other populations examined (Chinese, non-Chinese/non-Japanese Asian and non-Asian non-Caucasian). It would be interesting to determine whether or to what extent P450 levels and exposure to osimertinib and its active metabolites correlate with degree of clinical response, severity of side-effects, the emergence of resistance and disease progression, especially in light of our observation that, at a concentration which reflects that achieved clinically, this drug activates adaptive cellular stress responses which might alter its intracellular levels.

There are several indications that osimertinib may be suitable for first-line therapy of lung tumors; a low incidence of grade 3 or above adverse events (15), probable high levels of brain penetration with resultant enhanced efficacy over existing EGFR inhibitors for the treatment of metastases and leptomeningeal carcinomatosis (5,25,45,46), and, although the frequency is contentious, the pre-existence of T790M-positive clones in TKI-naïve EGFRm+ tumors (47). Moreover, there are many combination strategies involving osimertinib either proposed or in trial. As detailed above, *RAS* mutations are thought to confer resistance to osimertinib, which suggests a potential combination with MEK inhibitors (12). Other identified resistance mechanisms involve EGFR bypass through *HER2*/*ERBB2* or *MET* amplification/activation, similar to the T790M-unrelated mechanisms which occur in response to first generation inhibitors (12,13), and treatment with MET or EPHA2 inhibitors may be effective in these cases (48,49). Furthermore, although over-expression of ABCB1 in cell lines did not confer resistance to osimertinib, this compound inhibits ABCB1 activity and can enhance the efficacy of concomitantly administered cytotoxic agents (50). We posit that mice humanized for pathways of drug disposition can be used to model and predict drug/drug interactions prior to clinical trial. Such application would aid in the identification and prioritisation of the combination doses and schedules most likely to succeed in the clinic.

In conclusion, the data we have presented here will aid in the more effective deployment of osimertinib through pharmacologically-guided dose-adjustment. Moreover, with the ever-increasing molecular stratification of lung cancer suggesting further options for targeted intervention, and the expanding arsenal of targeted agents which might be combined with osimertinib, knowledge of its PK and DDI profiles will be essential for the pharmacologically-guided design of effective and tolerable combinations.

Acknowledgments

We thank Dr Yury Kapelyukh for conducting the EROD assay and Dr Shaohong Ding for carrying out the cell line work. We would also like to acknowledge Taconic Biosciences for the supply of the mouse lines used in this study. This work was supported by Cancer Research UK programme grant C4639/A10822.

References

1. GLOBOCAN_2012. http://globocan.iarc.fr/.
2. Shigematsu H, Lin L, Takahashi T, Nomura M, Suzuki M, Wistuba, II*, et al.* Clinical and biological features associated with epidermal growth factor receptor gene mutations in lung cancers. J Natl Cancer Inst **2005**;97:339-46
3. Paez JG, Janne PA, Lee JC, Tracy S, Greulich H, Gabriel S*, et al.* EGFR mutations in lung cancer: correlation with clinical response to gefitinib therapy. Science **2004**;304:1497-500
4. Pao W, Miller V, Zakowski M, Doherty J, Politi K, Sarkaria I*, et al.* EGF receptor gene mutations are common in lung cancers from "never smokers" and are associated with sensitivity of tumors to gefitinib and erlotinib. Proc Natl Acad Sci U S A **2004**;101:13306-11
5. Cross DA, Ashton SE, Ghiorghiu S, Eberlein C, Nebhan CA, Spitzler PJ*, et al.* AZD9291, an irreversible EGFR TKI, overcomes T790M-mediated resistance to EGFR inhibitors in lung cancer. Cancer Discov **2014**;4:1046-61
6. Sos ML, Rode HB, Heynck S, Peifer M, Fischer F, Kluter S*, et al.* Chemogenomic profiling provides insights into the limited activity of irreversible EGFR Inhibitors in tumor cells expressing the T790M EGFR resistance mutation. Cancer Res **2010**;70:868-74
7. Yun CH, Mengwasser KE, Toms AV, Woo MS, Greulich H, Wong KK*, et al.* The T790M mutation in EGFR kinase causes drug resistance by increasing the affinity for ATP. Proc Natl Acad Sci U S A **2008**;105:2070-5
8. Pao W, Miller VA, Politi KA, Riely GJ, Somwar R, Zakowski MF*, et al.* Acquired resistance of lung adenocarcinomas to gefitinib or erlotinib is associated with a second mutation in the EGFR kinase domain. PLoS Med **2005**;2:e73
9. Wu SG, Liu YN, Tsai MF, Chang YL, Yu CJ, Yang PC*, et al.* The mechanism of acquired resistance to irreversible EGFR tyrosine kinase inhibitor-afatinib in lung adenocarcinoma patients. Oncotarget **2016**;7:12404-13
10. astrazeneca-us.com. https://www.astrazeneca-us.com/media/press-releases/2016/TAGRISSO-osimertinib-met-primary-endpoint-in-phase-III-2nd-line-lung-cancer-trial-18072016.html.
11. Goss G, Tsai CM, Shepherd FA, Bazhenova L, Lee JS, Chang GC*, et al.* Osimertinib for pretreated EGFR Thr790Met-positive advanced non-small-cell lung cancer (AURA2): a multicentre, open-label, single-arm, phase 2 study. Lancet Oncol **2016**;17:1643-52
12. Ortiz-Cuaran S, Scheffler M, Plenker D, Dahmen L, Scheel AH, Fernandez-Cuesta L*, et al.* Heterogeneous Mechanisms of Primary and Acquired Resistance to Third-Generation EGFR Inhibitors. Clin Cancer Res **2016**
13. Planchard D, Loriot Y, Andre F, Gobert A, Auger N, Lacroix L*, et al.* EGFR-independent mechanisms of acquired resistance to AZD9291 in EGFR T790M-positive NSCLC patients. Ann Oncol **2015**;26:2073-8
14. Kim TM, Song A, Kim DW, Kim S, Ahn YO, Keam B*, et al.* Mechanisms of Acquired Resistance to AZD9291: A Mutation-Selective, Irreversible EGFR Inhibitor. J Thorac Oncol **2015**;10:1736-44
15. Janne PA, Yang JC, Kim DW, Planchard D, Ohe Y, Ramalingam SS*, et al.* AZD9291 in EGFR inhibitor-resistant non-small-cell lung cancer. N Engl J Med **2015**;372:1689-99
16. Brown K, Comisar C, Witjes H, Maringwa J, de Greef R, Vishwanathan K*, et al.* Population pharmacokinetics and exposure-response of osimertinib in patients with non-small cell lung cancer. Br J Clin Pharmacol **2017**;83:1216-26
17. Chakrabarti S, Michor F. Pharmacokinetics and drug-interactions determine optimum combination strategies in computational models of cancer evolution. Cancer Res **2017**

18. Pritchard MP, Ossetian R, Li DN, Henderson CJ, Burchell B, Wolf CR*, et al.* A general strategy for the expression of recombinant human cytochrome P450s in Escherichia coli using bacterial signal peptides: expression of CYP3A4, CYP2A6, and CYP2E1. Arch Biochem Biophys **1997**;345:342-54
19. Scheer N, Kapelyukh Y, Chatham L, Rode A, Buechel S, Wolf CR. Generation and characterization of novel cytochrome P450 Cyp2c gene cluster knockout and CYP2C9 humanized mouse lines. Mol Pharmacol **2012**;82:1022-9
20. Scheer N, Kapelyukh Y, McEwan J, Beuger V, Stanley LA, Rode A*, et al.* Modeling human cytochrome P450 2D6 metabolism and drug-drug interaction by a novel panel of knockout and humanized mouse lines. Mol Pharmacol **2012**;81:63-72
21. Hasegawa M, Kapelyukh Y, Tahara H, Seibler J, Rode A, Krueger S*, et al.* Quantitative prediction of human pregnane X receptor and cytochrome P450 3A4 mediated drug-drug interaction in a novel multiple humanized mouse line. Mol Pharmacol **2011**;80:518-28
22. Scheer N, McLaughlin LA, Rode A, Macleod AK, Henderson CJ, Wolf CR. Deletion of 30 murine cytochrome p450 genes results in viable mice with compromised drug metabolism. Drug Metab Dispos **2014**;42:1022-30
23. MacLeod AK, McLaughlin LA, Henderson CJ, Wolf CR. Activation Status of the Pregnane X Receptor Influences Vemurafenib Availability in Humanized Mouse Models. Cancer Res **2015**;75:4573-81
24. Wang XJ, Hayes JD, Wolf CR. Generation of a stable antioxidant response element-driven reporter gene cell line and its use to show redox-dependent activation of nrf2 by cancer chemotherapeutic agents. Cancer Res **2006**;66:10983-94
25. FDA_CPBR. http://www.accessdata.fda.gov/drugsatfda_docs/nda/.../208065Orig1s000ClinPharmR.pdf.
26. Dickinson PA, Cantarini MV, Collier J, Frewer P, Martin S, Pickup K*, et al.* Metabolic Disposition of Osimertinib in Rats, Dogs, and Humans: Insights into a Drug Designed to Bind Covalently to a Cysteine Residue of Epidermal Growth Factor Receptor. Drug Metab Dispos **2016**;44:1201-12
27. Forrester LM, Henderson CJ, Glancey MJ, Back DJ, Park BK, Ball SE*, et al.* Relative expression of cytochrome P450 isoenzymes in human liver and association with the metabolism of drugs and xenobiotics. Biochem J **1992**;281 (Pt 2):359-68
28. Drahushuk AT, McGarrigle BP, Larsen KE, Stegeman JJ, Olson JR. Detection of CYP1A1 protein in human liver and induction by TCDD in precision-cut liver slices incubated in dynamic organ culture. Carcinogenesis **1998**;19:1361-8
29. Ward RA, Anderton MJ, Ashton S, Bethel PA, Box M, Butterworth S*, et al.* Structure- and reactivity-based development of covalent inhibitors of the activating and gatekeeper mutant forms of the epidermal growth factor receptor (EGFR). J Med Chem **2013**;56:7025-48
30. McLellan LI, Wolf CR. Glutathione and glutathione-dependent enzymes in cancer drug resistance. Drug Resist Updat **1999**;2:153-64
31. EMA. http://www.ema.europa.eu/docs/en_GB/document_library/.../WC500202024.pdf.
32. FDA_PR. http://www.accessdata.fda.gov/drugsatfda_docs/nda/2015/208065Orig1s000PharmR.pdf.
33. McLemore TL, Adelberg S, Liu MC, McMahon NA, Yu SJ, Hubbard WC*, et al.* Expression of CYP1A1 gene in patients with lung cancer: evidence for cigarette smoke-induced gene expression in normal lung tissue and for altered gene regulation in primary pulmonary carcinomas. J Natl Cancer Inst **1990**;82:1333-9
34. Soria JC, Ohe Y, Vansteenkiste J, Reungwetwattana T, Chewaskulyong B, Lee KH*, et al.* Osimertinib in Untreated EGFR-Mutated Advanced Non-Small-Cell Lung Cancer. N Engl J Med **2018**;378:113-25
35. FDA_label. http://www.accessdata.fda.gov/drugsatfda_docs/label/2016/208065s002lbl.pdf.

36. Go RE, Hwang KA, Choi KC. Cytochrome P450 1 family and cancers. J Steroid Biochem Mol Biol **2015**;147:24-30
37. Butler MA, Lang NP, Young JF, Caporaso NE, Vineis P, Hayes RB*, et al.* Determination of CYP1A2 and NAT2 phenotypes in human populations by analysis of caffeine urinary metabolites. Pharmacogenetics **1992**;2:116-27
38. Schrenk D, Brockmeier D, Morike K, Bock KW, Eichelbaum M. A distribution study of CYP1A2 phenotypes among smokers and non-smokers in a cohort of healthy Caucasian volunteers. Eur J Clin Pharmacol **1998**;53:361-7
39. Zevin S, Benowitz NL. Drug interactions with tobacco smoking. An update. Clin Pharmacokinet **1999**;36:425-38
40. O'Malley M, King AN, Conte M, Ellingrod VL, Ramnath N. Effects of cigarette smoking on metabolism and effectiveness of systemic therapy for lung cancer. J Thorac Oncol **2014**;9:917-26
41. Hughes AN, O'Brien ME, Petty WJ, Chick JB, Rankin E, Woll PJ*, et al.* Overcoming CYP1A1/1A2 mediated induction of metabolism by escalating erlotinib dose in current smokers. J Clin Oncol **2009**;27:1220-6
42. Das M, Padda SK, Frymoyer A, Zhou L, Riess JW, Neal JW*, et al.* Dovitinib and erlotinib in patients with metastatic non-small cell lung cancer: A drug-drug interaction. Lung Cancer **2015**;89:280-6
43. Planchard D, Brown KH, Kim DW, Kim SW, Ohe Y, Felip E*, et al.* Osimertinib Western and Asian clinical pharmacokinetics in patients and healthy volunteers: implications for formulation, dose, and dosing frequency in pivotal clinical studies. Cancer Chemother Pharmacol **2016**;77:767-76
44. Tateishi T, Watanabe M, Nakura H, Asoh M, Shirai H, Mizorogi Y*, et al.* CYP3A activity in European American and Japanese men using midazolam as an in vivo probe. Clin Pharmacol Ther **2001**;69:333-9
45. Ballard P, Yates JW, Yang Z, Kim DW, Yang JC, Cantarini M*, et al.* Preclinical Comparison of Osimertinib with Other EGFR-TKIs in EGFR-Mutant NSCLC Brain Metastases Models, and Early Evidence of Clinical Brain Metastases Activity. Clin Cancer Res **2016**
46. Nanjo S, Ebi H, Arai S, Takeuchi S, Yamada T, Mochizuki S*, et al.* High efficacy of third generation EGFR inhibitor AZD9291 in a leptomeningeal carcinomatosis model with EGFR-mutant lung cancer cells. Oncotarget **2016**;7:3847-56
47. Ye X, Zhu ZZ, Zhong L, Lu Y, Sun Y, Yin X*, et al.* High T790M detection rate in TKI-naive NSCLC with EGFR sensitive mutation: truth or artifact? J Thorac Oncol **2013**;8:1118-20
48. Ou SH, Agarwal N, Ali SM. High MET amplification level as a resistance mechanism to osimertinib (AZD9291) in a patient that symptomatically responded to crizotinib treatment post-osimertinib progression. Lung Cancer **2016**;98:59-61
49. Amato KR, Wang S, Tan L, Hastings AK, Song W, Lovly CM*, et al.* EPHA2 Blockade Overcomes Acquired Resistance to EGFR Kinase Inhibitors in Lung Cancer. Cancer Res **2016**;76:305-18
50. Hsiao SH, Lu YJ, Li YQ, Huang YH, Hsieh CH, Wu CP. Osimertinib (AZD9291) Attenuates the Function of Multidrug Resistance-Linked ATP-Binding Cassette Transporter ABCB1 in Vitro. Mol Pharm **2016**;13:2117-25

Figure 1. Species comparison of osimertinib metabolites generated in liver microsomal fractions *in vitro*. Incubations were carried out with mouse or human liver microsomal fractions as described in the Materials and Methods. Using pooled HLM, two peaks corresponding to demethylated products **(A)** and five peaks corresponding to hydroxylated products **(B)** were detected. With wild-type MLM, two demethylated **(C)** and two hydroxylated **(D)** products predominated. **(E)** Demethylated forms were generated at similar levels by HLM and MLM, whereas hydroxylated forms were more species-specific. In **A-D**, abundance is calculated relative to base peak signal whereas, in **E**, abundance is calculated relative to internal standard. Data shown are mean ± SD of triplicate incubations. **(F)** Structure of osimertinib showing sites of metabolism, characterised and as shown in more detail in **Supplementary Figure 1**.

Figure 2. *In vitro* metabolism of osimertinib by a panel of recombinant human cytochrome P450s. Osimertinib was incubated with recombinant P450 as described in the Materials and Methods and conversion to **(A)** DM-1, **(B)** DM-2, **(C)** OH-1, **(D)** OH-2, **(E)** OH-3, **(F)** OH-4 and **(G)** OH-5 forms measured by LC-MS/MS. Data shown are mean ± SD of triplicate incubations and are representative of three separate experiments.

Figure 3. The profound species difference in osimertinib disposition relates to metabolism by murine Cyp2d enzymes. (A) Metabolic stability of osimertinib in pooled HLM and MLM from WT and P450-knockout mice. Formation of **(B)** OH-2 was monitored in the same incubations. Data shown are mean ± SD of triplicate incubations and are representative of three separate experiments. Wild-type and h2D6 animals were administered osimertinib (25 mg/kg *p.o.*) and blood samples collected at the indicated timepoints for measurement of **(C)** osimertinib and **(D)** OH-2-osimertinib. Data shown are mean ± SD with n = 4 in each group. Apparent PK parameters are detailed in **Supplementary Table 4**.

Figure 4. CYP3A4 mediates osimertinib metabolism in humanised mice. hPXR/hCAR/3aKO and hPXR/hCAR/h3A4 animals were administered rifampicin (10 mg/kg *i.p.*) or corn oil vehicle once daily for three days then, on day four, osimertinib (25 mg/kg *p.o.*). Blood samples were collected at the indicated timepoints after osimertinib administration for measurement of **(A,B)** osimertinib, **(C,D)** DM-1-osimertinib, and **(E,F)** DM-2-osimertinib. Data shown are mean ± SD with n = 4 in each group. Apparent PK parameters are detailed in **Supplementary Table 5**.

Figure 5. Osimertinib is a substrate and inducer of CYP1A1 *in vivo*. h1A1/1A2 and 1a1/1a2KO animals were administered TCDD (10 µg/kg *i.p.*) or corn oil vehicle on day one and osimertinib (25 mg/kg *p.o.*) on day three. Blood samples were collected at the indicated timepoints after osimertinib administration for measurement of **(A)** osimertinib and **(B)** OH-1-osimertinib. Data shown are mean ± SD with n = 4 in each group. Apparent PK parameters are detailed in **Supplementary Table 6**. Formation of **(C)** OH-1, **(D)** OH-3 and **(E)** OH-5 was monitored in incubations with lung microsomes from WT, h1A1/1A2, and Cyp1aKO animals with/without TCDD-pretreatment. Data shown are mean ± SD of triplicate incubations. In a separate experiment, h1A1/1A2 animals were administered vehicle or osimertinib (25 mg/kg *p.o.*) once daily for four days. On day five, livers were harvested and CYP1A1 levels assessed by Western blotting **(F)** and 7-ethoxyresorufin-O-deethylase activity **(G)** (p=0.027, unpaired t test).

Author Manuscript Published OnlineFirst on February 6, 2018; DOI: 10.1158/1078-0432.CCR-17-3555
Author manuscripts have been peer reviewed and accepted for publication but have not yet been edited.

Figure 1

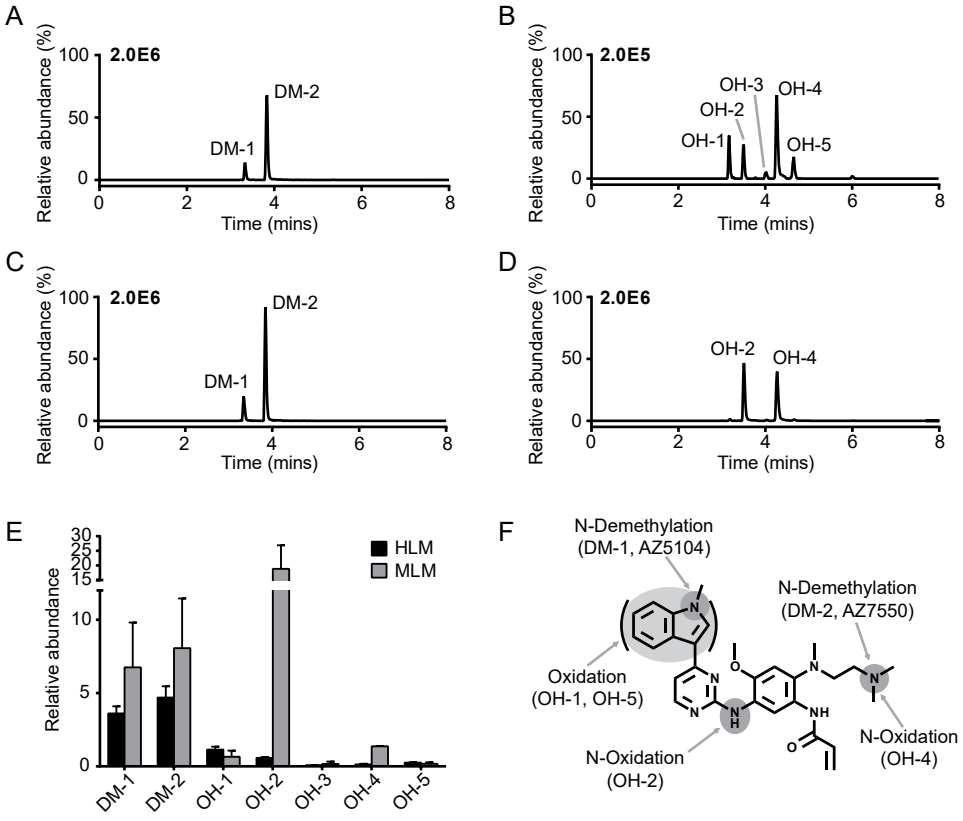

Author Manuscript Published OnlineFirst on February 6, 2018; DOI: 10.1158/1078-0432.CCR-17-3555
Author manuscripts have been peer reviewed and accepted for publication but have not yet been edited.

Figure 2

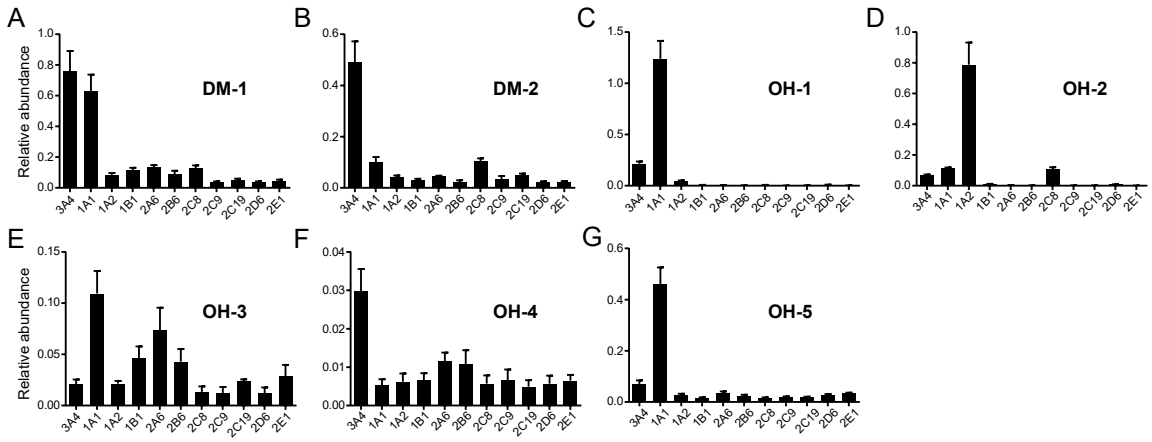

Author Manuscript Published OnlineFirst on February 6, 2018; DOI: 10.1158/1078-0432.CCR-17-3555
Author manuscripts have been peer reviewed and accepted for publication but have not yet been edited.

Figure 3

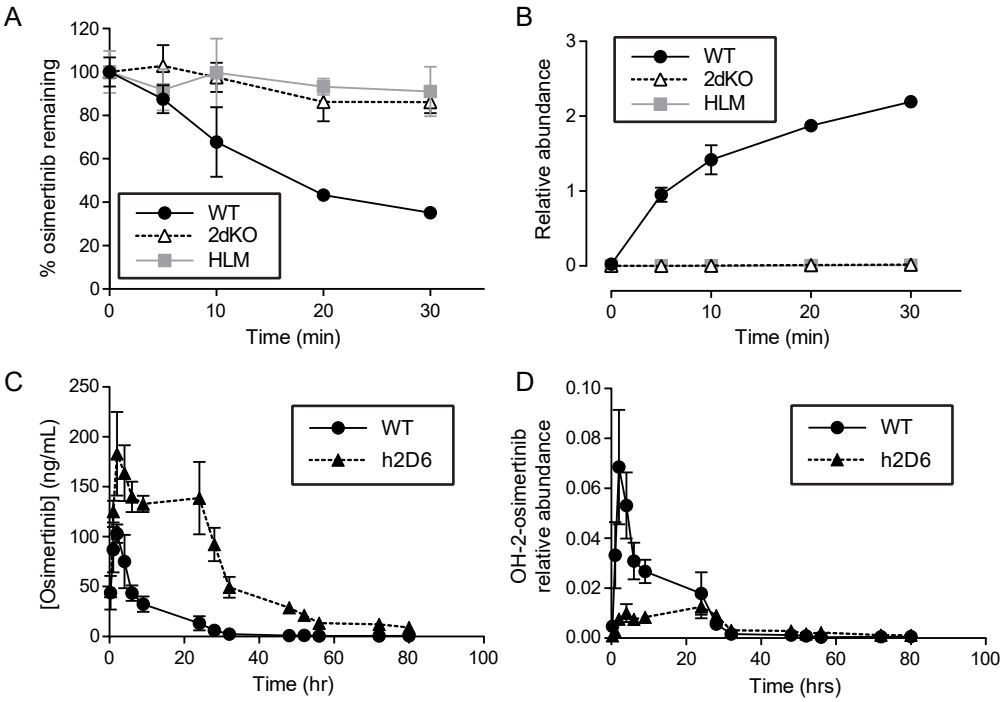

Author Manuscript Published OnlineFirst on February 6, 2018; DOI: 10.1158/1078-0432.CCR-17-3555
Author manuscripts have been peer reviewed and accepted for publication but have not yet been edited.

Figure 4

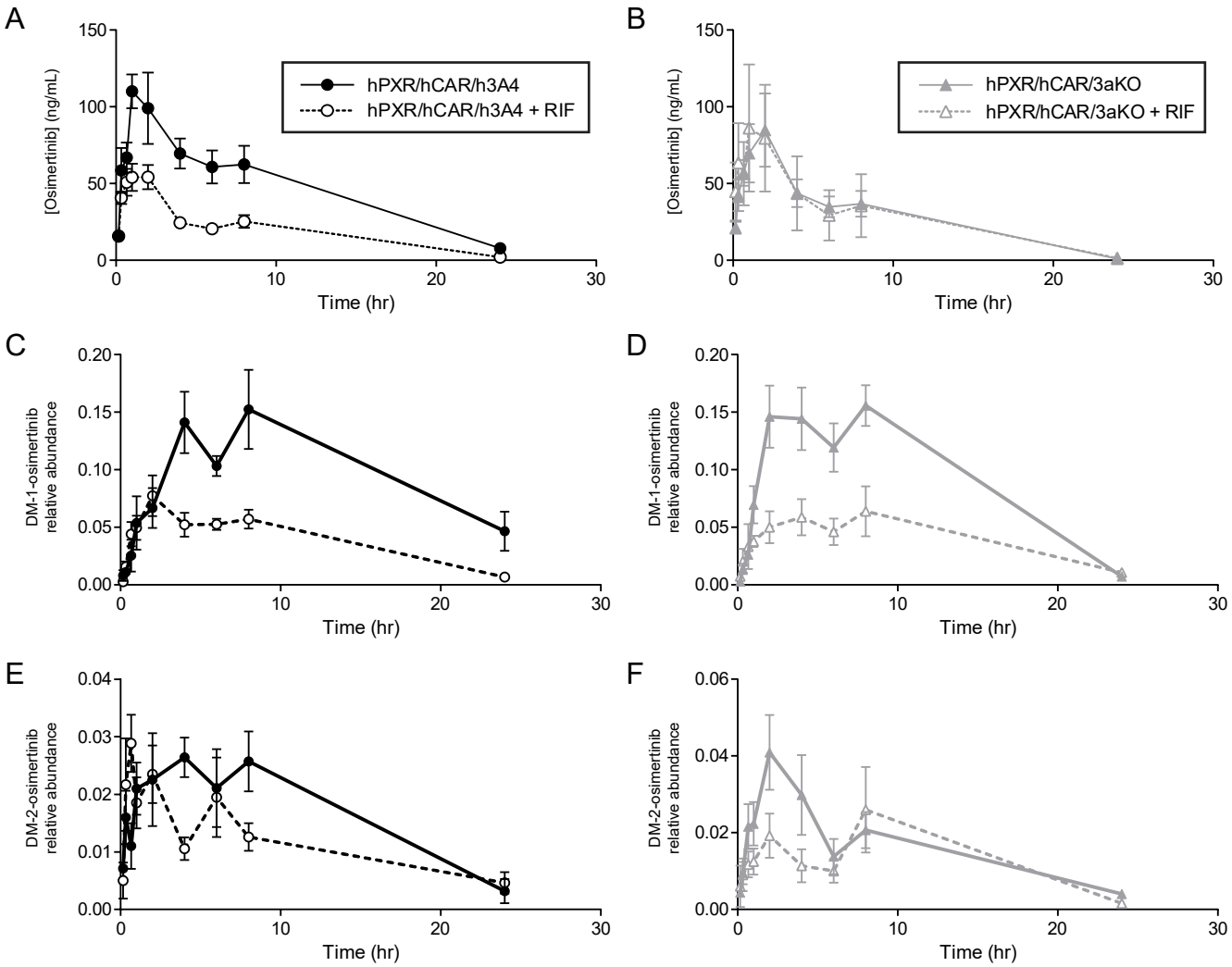

Author Manuscript Published OnlineFirst on February 6, 2018; DOI: 10.1158/1078-0432.CCR-17-3555
Author manuscripts have been peer reviewed and accepted for publication but have not yet been edited.

Figure 5

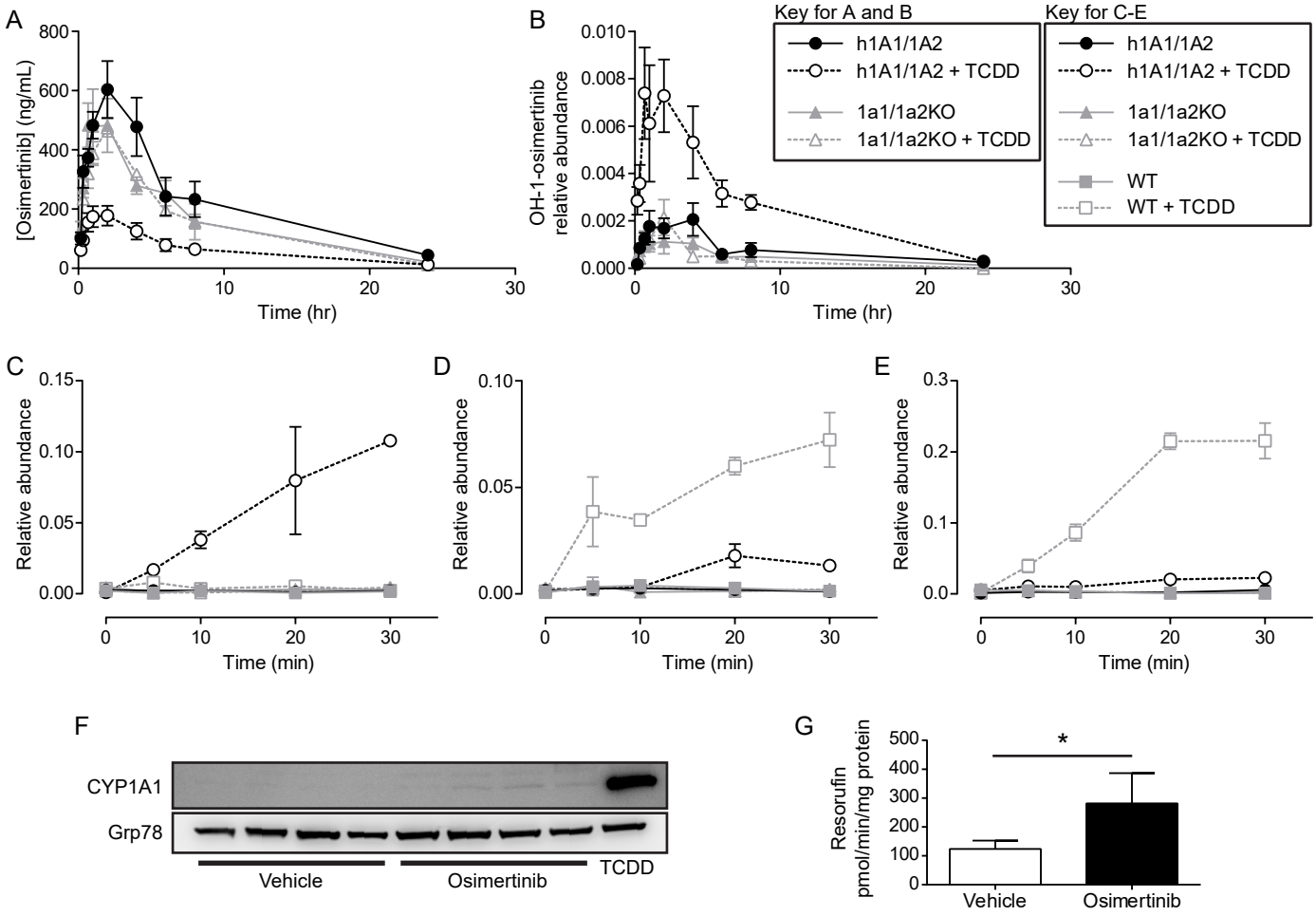

AACR American Association for Cancer Research

Clinical Cancer Research

Identification of novel pathways of osimertinib disposition and potential implications for the outcome of lung cancer therapy

A. Kenneth MacLeod, De Lin, Jeffrey T.-J. Huang, et al.

Clin Cancer Res Published OnlineFirst February 6, 2018.